

Temperature Dependent Polarization Effect and Capacitive Performance Enhancement of PVA-Borax Gel Electrolyte

S. Demirel

Igdir University, Electricity and Energy Department, 76002 Igdir, Turkey

E-mail: serkan.demirel@igdir.edu.tr

Received: 13 November 2019 / Accepted: 14 January 2020 / Published: 10 February 2020

In this paper the space-polarization effect and capacitive performance enhancement have been reported of Polyvinyl Alcohol (PVA)-Borax gel electrolyte. To improve structural and electrochemical performance the anionic Cl^- and cationic Na^+ were doped into PVA-Borax system via NaCl salt. The structural studies showed that there is no any impurity phase formation in PVA-Borax structure with NaCl dopes. It was determined that NaCl dopes affect the $\text{B}(\text{OH})_4^-$ anionic structure in the PVA-Borax system. As a result of electrochemical CV measurements, in (-1) - (+1) voltage range, the samples showed rectangular shape current property as a supercapacitor electrolyte. According to capacitance results, the highest capacitance value was obtained as 0.082 F g^{-1} with 5 mmol NaCl doped sample at room temperature. In the long cycle life measurements, 1 mmol NaCl doped sample showed more stable capacitance behavior. The temperature depending capacitance measurements showed that the PVA-Borax gel electrolyte has space-polarization effect. Also, both anionic and cationic dopes via NaCl has a positive effect on capacitive performance of PVA-Borax gel electrolyte and it provides advantages to technological capacitor applications.

Keywords: PVA-Borax, anionic dope, cationic dope, supercapacitor.

1. INTRODUCTION

Thin, smaller, lighter, flexible, wearable and higher temperature capability technologies need to novel electronic components. In these components, the energy storage devices play the most important role [1-3]. Over half a century, R&D studies have been continuing to produce higher performance and more reliable energy storage systems.

It is great importance to develop the electrolyte materials may solve some problems in terms of security for energy storage systems [1,4,5]. Electrolyte materials that can be synthesized as liquid, solid and gel types are used in various technological applications according to their performance and properties [3,6,7]. The liquid electrolytes generally have high capacitive performance. However, they require to use extra special ionic permeable membranes due to their high electric conductivity, and

prevent the short-circuit between two electrodes [7, 8]. Also, some liquid electrolytes much more toxic and harmful for environment. On the other hand, the solid type electrolytes do not require membranes due to their high dielectric structure, and, it is much safer than liquid electrolytes [9]. But it has big disadvantages as capacitive performance due to low electrolyte-electrode interaction [9]. The gel type electrolytes are located between these two types electrolytes in terms of performance and safety. It is better than solid electrolytes in terms of capacitive performance and better than liquid electrolytes in terms of safety. It also has some advantages in technological applications. High electrode-electrolyte surface interaction, electrochemical stabilization, ideal electrical and ionic conductivity coefficient, non-use of membranes, easily synthesis, usability in air etc [7-10].

Among the gel electrolytes that can be synthesized with different materials, the most remarkable one is the polymer-based gel electrolytes. In particular, non-toxic and water-soluble polyvinyl alcohol (PVA) and polyethylene oxide (PEO), Poly Acrylonitrile (PAN) and Poly Methyl Methacrylates (PMMA) are used as the main materials [11-13]. Also, those polymers have some advantages like solvate large amount of electrolyte salts, high ionic conductivities, high mechanical strengths [11-13]. According to some research studies, the anionic and cationic dopes like (F^- , Cl^- , SiO_4^{-4} , CO_2^{-3} , Na^+ , Mg^{2+} , K^+ , Sr^{2+} , Zn^{2+} , Ba^{2+} , Al^{3+}) are so important for both material structure stabilization and electrochemical enhancements [14-17].

Above in these polymers, the PVA is the most unique material for technological device applications like electrochromism, energy storage systems etc. It can be easily converted gel form with Borax or boric acid, as non-toxic and environmentally friendly. Especially, the PVA-Borax gel is used in electrochemical energy storage devices as high energy storage electrolyte materials [18-20].

Even if the high energy storage and stability are so important factors in the new generation technological products, temperature depending performance stability is also so important [21]. Under normal conditions, the dielectric coefficient of a capacitor increases depending on the temperature increase, but in some cases, it may fall despite the temperature increase [22,23]. The most important factor of this situation, oxygen vacancies and ion mobilization increase in the structure. This is known as space polarization effect [24].

Generally, this study aims to PVA-Borax gel electrolyte performance enhancements for both electrochemical and high temperature applications. In experimental studies, NaCl salts has been used to both anionic and cationic dopes in PVA-Borax system (cationic Na^+ and anionic Cl^-), profit by distilled water and PVA's large amount of electrolyte salts solving advantage. The structural changes have been observed via FTIR analysis. Also, electrochemical capacitance performance and temperature stability properties were investigated of PVA-Borax gel and NaCl doped sample electrolytes for supercapacitor applications. In addition, temperature depending capacitance properties were examined for technological applicability in daily life technology.

2. EXPERIMENTAL

Figure 1 shows PVA-Borax gel electrolyte synthesis schematic. To synthesis gel electrolyte, 97% purity polyvinyl alcohol (PVA), high purity distilled water, commercial borax ($Na_2[B_4O_5(OH)_4] \cdot 8H_2O$) and 97% purity NaCl were used. In the first stage, homogenous gel was produced by mixing distilled

water and 4% PVA at 70 °C for 1 hour. In this process, applied heat accelerates the solubility of PVA in water and ensures that the mixture becomes a gel. Afterwards, 4% Borax-distilled water solution was prepared at room temperature. In the final stage of PVA-Borax gel fabrication, 0.5 ml Borax solution was added to 5 ml of PVA gel and mixed at room temperature.

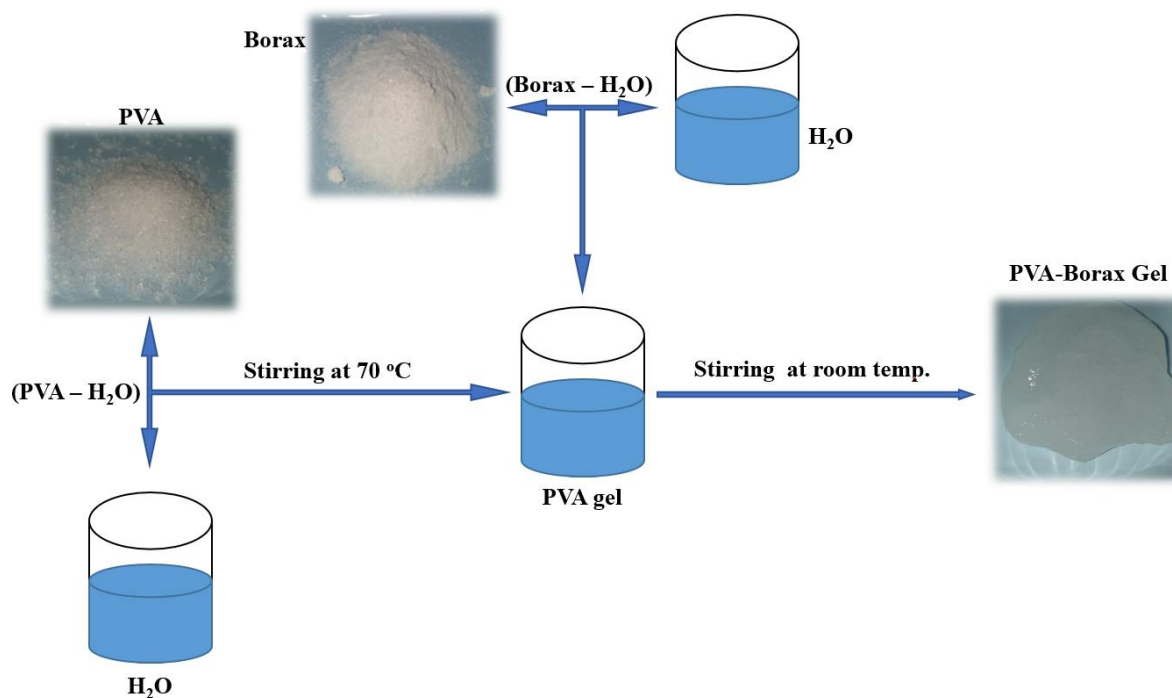


Figure 1. Schematic of PVA-Borax gel electrolyte synthesis.

To synthesis of NaCl doped gel electrolyte samples, 1 mmol and 5 mmol NaCl powders were weighed and doped to the PVA gel. To obtain homogeneous PVA-NaCl gel, the solution was stirred about 15 minutes at room temperature. After this process, 0.5 ml Borax solution was added to PVA-NaCl samples and PVA-Borax-NaCl gel samples were produced.

To structural analysis, FTIR measurement was used to clearly see the structural changes of samples. The Shimadzu brand FTIR spectrometer system was used, and, the FTIR measurements has been conducted from 600 to 2000 cm^{-1} wavenumbers.

Wheestat portable potentiostat was used for electrochemical measurements. The cyclic voltammetry (cv) measurements were performed in 3 cell electrode system in a 20 ml chemical cell. Commercial graphite rods of the same dimensions were used as electrodes in the measurements. CV measurements were performed at constant scanning speeds of 100, 200 and 400 mV s^{-1} . The specific capacitance calculations were made with 100 mV s^{-1} constant scanning rate cv measurement results by using the following formula [24, 25];

$$C = \frac{\int I \cdot dv}{2 \cdot m \cdot \Delta V \cdot v} \quad (1)$$

where, I ; current, m ; weight of the active material, v ; scan rate, ΔV ; potential window. The temperature depending capacitance measurements were made in 20-90 °C range using $\pm 1^\circ\text{C}$ precision temperature adjustable heat chamber. The dielectric coefficient calculated with obtained capacitance values by following formula [30];

$$C = \frac{\epsilon_0 A}{d} \quad (2)$$

where, C ; capacitance, A ; area of plate, d ; distance between two plates, ϵ_0 ; dielectric constant. The capacitance fade calculation has been made between room temperature and at 80 °C capacitance results by following formula;

$$\text{Fade}(\%) = \frac{(C_0 - C_t)}{C_0} \times 100 \quad (3)$$

where; C_0 ; room temperature capacitance value, C_t ; 80 °C capacitance value.

3. RESULTS

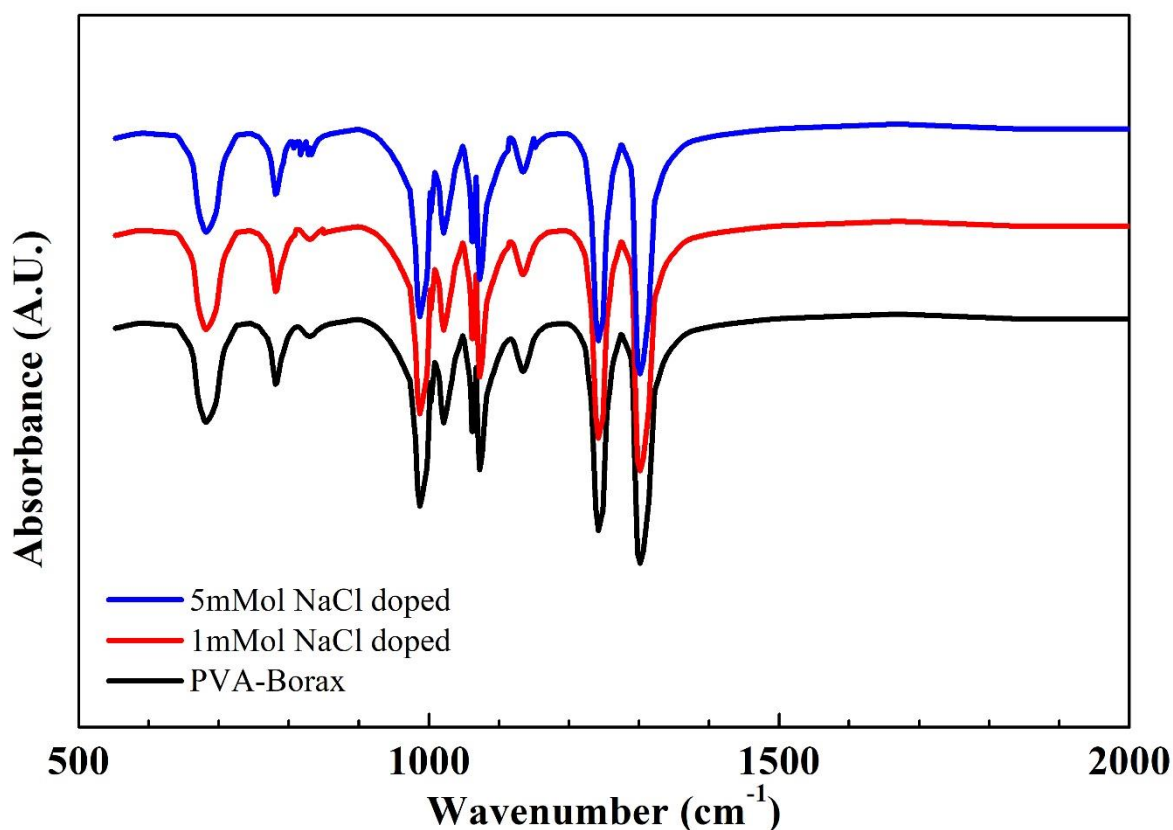


Figure 2. FTIR analysis of PVA-Borax and NaCl doped gel electrolytes.

Figure-2 shows the FTIR analysis of PVA-Borax gel and NaCl doped samples. It was determined that FTIR analysis was generally compatible with literature [22, 23]. As a result of literature research 1241 cm^{-1} and 1303 cm^{-1} peaks correspond to asymmetric stretching relaxation of B-O-C bonds, 831 cm^{-1} peak corresponds to B-O stretching from residual $\text{B}(\text{OH})_4^-$, and, 682 cm^{-1} peak correspond to bending of B-O-B linkages within borate networks [28]. According to FTIR analyses, it was determined that 5 mmol NaCl doped caused degradation of the structure at the peak of 831 cm^{-1} . It was determined that this peak corresponds to $\text{B}(\text{OH})_4^-$ anions in PVA-Borax structure, and, anionic Cl^- dopig is caused disrupting $\text{B}(\text{OH})_4^-$ structure [22]. Apart from this deterioration, NaCl dopes did not cause any impurity phase formations in PVA-Borax structure.

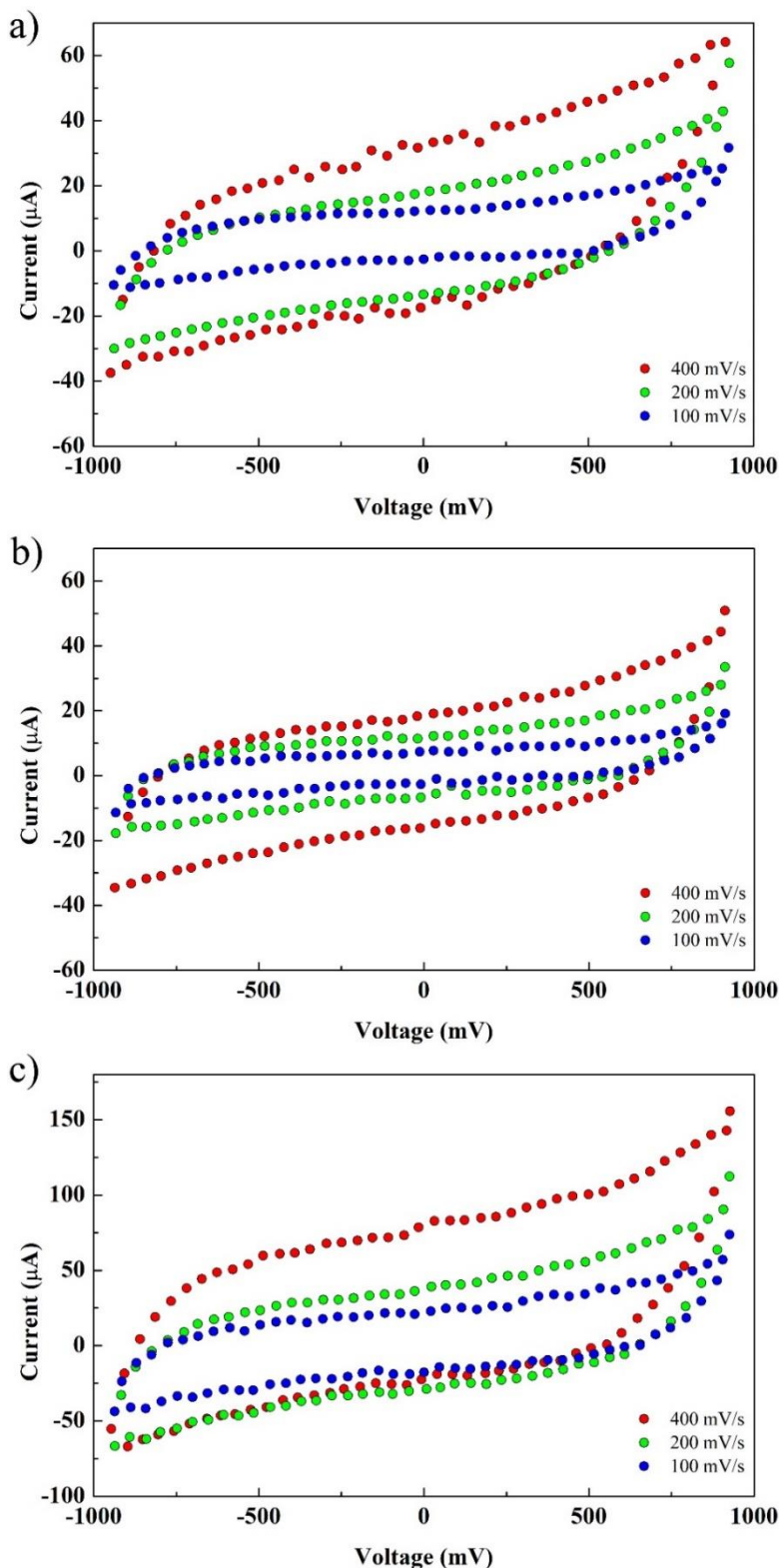


Figure 3. CV analysis of gel electrolyte samples a) Pure PVA-Borax gel electrolyte, b) 1 mmol NaCl doped gel electrolyte, c) 5 mmol NaCl doped gel electrolyte.

Figure 3 shows cv measurements for PVA-Borax and NaCl doped samples. In this stage, the cv measurements have been taken as 3 cycles for each scan rate and for each sample. To clear see and

comparing of different scan rates results, only one cycle results gave in figure 3 for each sample. According to cv measurement results, the samples have showed capacitive currents plateaus in negative and positive regions during 3 cycles for each scan rate. It supports the PVA-Borax and NaCl doped gel samples shows rechargeable electrolyte property for capacitors. Figures 3-b shows that cv measurements become more clearly rectangular shape with 1 mmol NaCl dope. According to literature which is specific characteristic for a supercapacitor [26, 29]. In Figure 3-c, it is observed that there is an abnormal increase in positive current region especially with increasing NaCl doping. When this region is examined together with FTIR results, it is caused by the deterioration in $B(OH)_4^-$ by Cl^- anions and the increase of cationic Na^+ and B^{+3} ions in the structure.

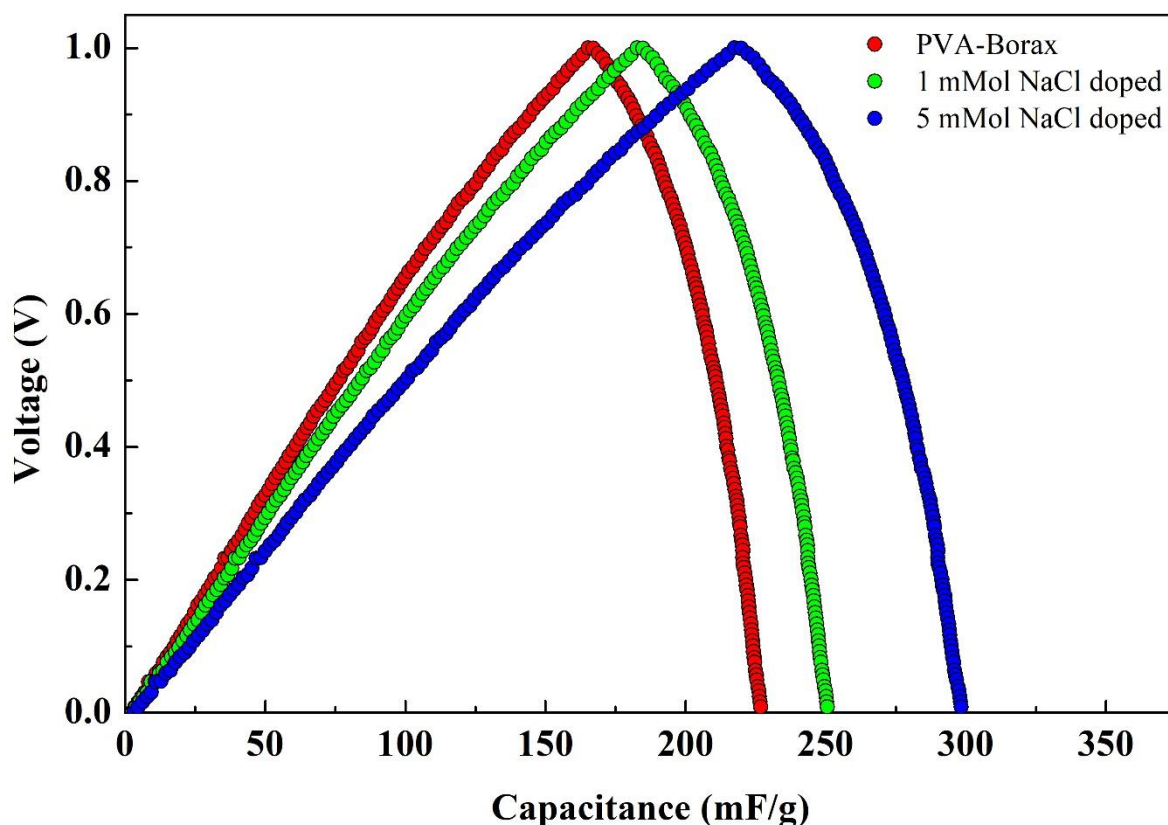


Figure 4. First cycle capacitance results for gel electrolytes.

Figure 4 shows the capacitance results for the first cycle in the 0-1V range. At the end of the first cycle, the discharge capacitances were determined to be 0.061 F g^{-1} for PVA-Borax, 0.067 F g^{-1} for 1 mmol, and, 0.082 F g^{-1} for 5 mmol NaCl dopes. It is seen that the number of released electrons increases in the PVA-Borax structure with the NaCl dopes. As a result of it, the capacitance increases in charge and discharge regions. Figure-5 shows the charge-discharge cyclic performance of gel electrolyte samples. Although the highest capacity was obtained in the 5 mmol NaCl doped sample, the high-performance stability was obtained by 1 mmol NaCl doped samples in long cycle process. In particularly, the capacitance equilibrated as $\sim 21 \text{ mF g}^{-1}$ for pure PVA-Borax and 5 mmol NaCl doped samples, while this level was $\sim 28 \text{ mF g}^{-1}$ in 1 mmol doped sample at the end of 10 cycles.

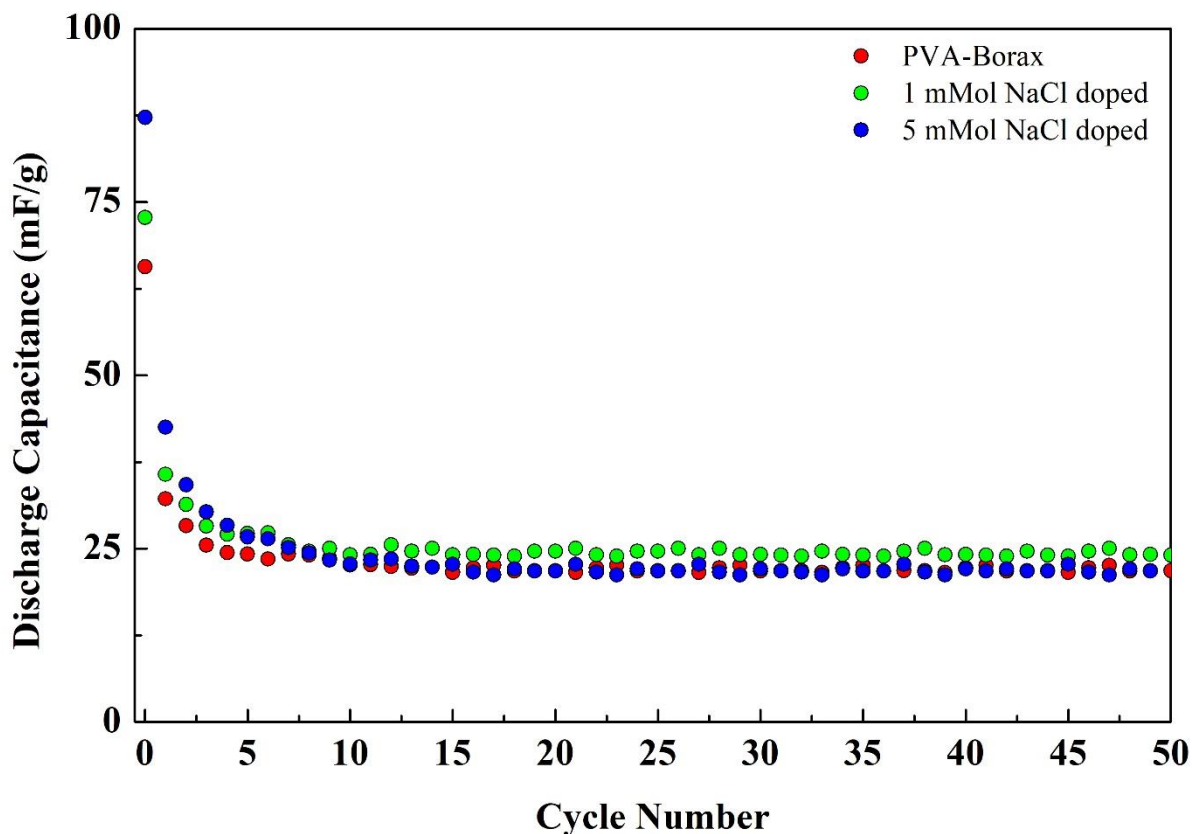


Figure 5. Discharge capacitance performance of gel electrolytes.

Figure 6-a shows the temperature dependent capacitance results. According to results, a certain increase is seen in capacitance up to 40 °C, while it is seen that capacitance values decreasing in 40-80 °C temperature range. Under normal conditions, temperature increases cause to capacitance increases depending on the increasing dielectric coefficient [22]. However, in this study the capacitance decreasing in 40-80 °C, and, it may be caused by space polarization effects with increasing oxygen vacancies in the aqueous PVA-Borax structure. According to Singh et al. study this anomaly explains as “dielectric loss may be the space charge polarization coming from mobile ions which in present case could be the oxygen vacancies” [27]. Similar effect can be caused from weak $B(OH)_4^-$ anions and Na^+ cations in Borax structure. It is thought that increasing temperature weakens the oxygen bonds in aqueous PVA-Borax structure, and, it causes to increase of oxygen vacancies. As a result of the space polarization effect, electrical conductivity increased and dielectric coefficient decreased by mobile ions and oxygen vacancies [23, 27]. When capacity values are examined, 5mmol NaCl doping sample has reached the highest discharge capacitance value with $\sim 89 \text{ mF g}^{-1}$, 1 mmol NaCl doped sample reached $\sim 80 \text{ mF g}^{-1}$, and, pure PVA-Borax capacitance remained at $\sim 72 \text{ mF g}^{-1}$ at 40 °C. The values obtained at 80 °C were 66, 62 and 53 mF g^{-1} for pure sample, 1 mmol NaCl and 5 mmol NaCl, respectively.

The calculated capacitance fade percentages for pure sample, 1 mmol NaCl and 5 mmol NaCl are 19.5%, 7.46% and 13.11%, respectively.

Table 1. Gel electrolyte comparisons.

Electrolyte	Capacitance (mFg ⁻¹)	Working Potential (V)	Ref.
Propylene Carbonate (PC)-2-hydroxyethyl methacrylate (HEMA)	74	0-(1.2)	[31]
Polyvinyl Alcohol (PVA)-H ₂ SO ₄ -H ₂ O	38.5	0-1	[32]
Polyvinyl Alcohol (PVA)-H ₃ PO ₄ -H ₂ O	95	0-1	[33]
Polyvinyl Alcohol (PVA)-Borax	72	0-1	This study
Polyvinyl Alcohol (PVA)-Borax-NaCl	82	0-1	This study

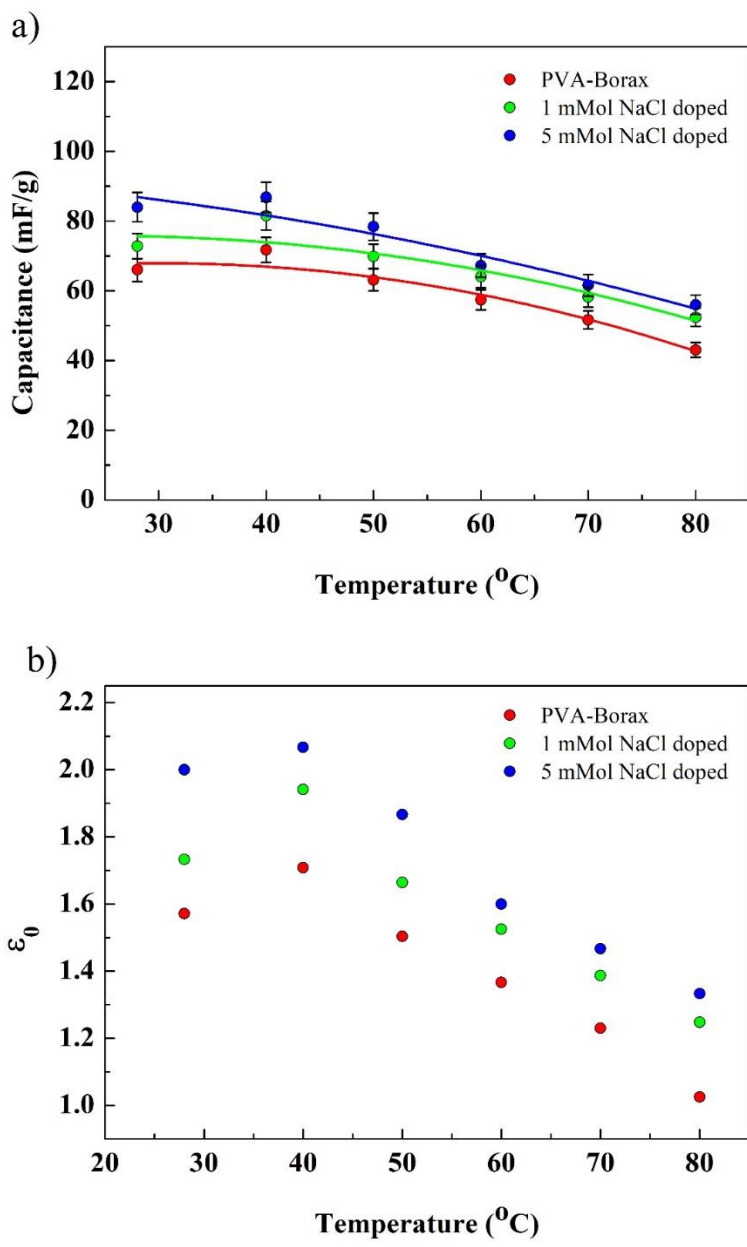


Figure 6. a) Temperature depending discharge capacitance values, b) Temperature depending calculated dielectric constants.

Table 1 shows the capacitance comparisons of different gel electrolytes for supercapacitors under similar conditions [31-33]. According to capacitive performance comparisons, PVA-Borax gel electrolyte better than PVA-H₂SO₄-H₂O and PC-HEMA gel electrolytes [31, 32]. Besides, this study shows that the ionic doped PVA-Borax gel electrolyte capacitive performance can be reached of other good performance gel electrolytes.

Figure 6-b shows the dielectric coefficients, which calculated from capacitance measurement results. When Figure 6-b is examined, it is seen that dielectric coefficient increases up to 40 °C with increasing temperature. However, despite the increasing temperature between 40-80 °C, the electrical conductivity increases in the structure. In particular, this trend is similar in both pure and NaCl-doped samples, and, it supports the space polarization effect in the structure.

4. CONCLUSION

The PVA-Borax gel electrolyte and NaCl doped samples were synthesized successfully. There is no any impurity phases formation with NaCl doping, however, it was determined that the NaCl dopes cause to deterioration of the B(OH)₄⁻ anionic structure by Cl⁻ anion. The electrochemical cyclic voltammetry (cv) measurements showed that the samples have rectangular shape current in the range of (-1)V - (+ 1)V. According to this result, PVA-Borax gel electrolyte and NaCl doped samples can be suitable for use as supercapacitor gel electrolyte. When the capacitance results were compared, it was determined that the 5 mmol NaCl doped samples have the highest capacitance value in the first cycle. The long cycle measurement results have showed that the 1 mmol NaCl doped samples are more stable and have higher capacitance values than other samples. Also, 1 mmol NaCl doped samples more efficient than other samples with 7.46% capacitance fade in 25-80 °C temperature range. The temperature depending capacitance measurements showed that PVA-Borax structure shows space polarization effect after 40 °C. The dielectric loss by space polarization effect can be use some temperature-dependent sensor applications. As result, 1 mmol NaCl dopes enhanced both the electrochemical and temperature dependent performances of PVA-Borax gel electrolyte, and, it was found to be more advantageous for technology.

ACKNOWLEDGEMENT

This study was supported by Iğdir University-Scientific Research Projects Coordination Unit project no:2019-FBE-A23.

References

1. Q. Chen, X. Li, X. Zang, Y. Cao, Y. He, P. Li, K. Wang, J. Wei, D. Wu and H. Zhu, *RSC Adv.*, 4 (2014) 36253.
2. M. S. Kumar, M. C. Rao, *Mater. Res. Express*, 6 (2018) 039502.
3. J. Chojnacka, L. J. Acosta, E. Morales, *Power Sour.*, 97-98 (2001) 819.
4. M. Saraf, K. Natarajan, A. K. Gupta, P. Kumar, R. Rajak and S. M. Mobin, *Mater. Res. Express*, 6 (2019) 095534.

5. P. Venkatachalam, T. Kesavan, G. Maduraiveeran, M. Kundu and M. Sasidharan, *Mater. Res. Express*, 6 (2018) 035502.
6. L. Rita, R. Patrícia, S. Rodrigo, R. Leandro, D. A. S. Igor, C. Andrea, D. Jose, M. Claudio, E. José, P. Agnieszka, M. Silva, *Electrochim. Acta*, 240 (2017) 474.
7. Q. Tan, P. Irwin, Y. Cao, *IEEJ Transactions on Fundamentals and Materials*, 126 (2006) 1153.
8. X. Lin, M. Salari, L. M. R. Arava, P. M. Ajayan and M.W. Grinstaff, *Chem. Soc. Rev.*, 45 (2016) 5848.
9. S. Choudhury, S. Stalin, D. Vu, A. Warren, Y. Deng, P. Biswal and L. A. Archer, *Nat. Comm.*, 10 (2019) 4398.
10. B. Pal, S. Yang, S. Ramesh, V. Thangadurai and R. Jose, *Nanoscale Adv.*, 1 (2019) 3807.
11. P. K. Varshney and S. Gupta, *Ionics*, 17 (2011) 479.
12. H. T. T. Thanh, P. A. Le, M. D. Thi, T. L. Quang and T. N. Trinh, *Bull. Mater. Sci.*, 41 (2018) 145.
13. D. Kumar, H. Wadhwa, S. Mahendia, F. Chand and S. Kumar, *Mater. Res. Express*, 4 (2017) 025021.
14. B. Wang, J. A. Macia-Agullo, D. G. Prendiville, X. Zheng, D. Liu, Y. Zhang, S. W. Boettcher, X. Ji, and G. D. Stucky, *J. Electrochem. Soc.*, 2014, 161, A1090.
15. Y. Li, X. Cai, W. Shen, *Electrochim. Acta*, 149 (2014) 306.
16. I. Cacciotti, *J. Appl. Ceram. Technol.*, 16 (2019) 1864.
17. I. Cacciotti, *Handbook of Bioceramics and Biocomposites*. Berlin, Germany: Springer International Publishing (2016) 145.
18. Y. Alesanco, J. Palenzuela, A. Vinuales, G. Cabanero, H. J. Grande, and I. Odriozola, *ChemElectroChem*, 2 (2015) 218.
19. M. Jiang, J. Zhu, C. Chen, Y. Lu, Y. Ge, X. Zhang, *ACS Appl. Mater. Interfaces*, 8 (2016) 3473.
20. Z. Wang, F. Tao and Q. Pan, *J. Mater. Chem. A*, 4 (2016) 17732.
21. H. Chen, T. N. Cong, W. Yang, C. Tan, Y. Li, Y. Ding, *Pro. Nat. Sci.*, 19 (2009) 291.
22. V. S. Yadav, D. K. Sahu, Y. Singh, D. C. Dhubbkarya, *Proceedings of the International Multi Conference of Engineers and Computer Scientists*, (2010) DOI: 10.1063/1.3510553
23. T-F. Zhang, X-G. Tang, Q-X. Liu, S-G. Lu, Y-P. Jiang, X-X. Huang, and Q-F. Zhou, *AIP Adv.*, 4 (2014) 107141.
24. X. L. Guo, X. Y. Liu, X. D. Hao, S. J. Zhu, F. Dong, Z. Q. Wen, Y. X. Zhang, *Electrochim. Acta*, 194 (2016) 179.
25. H. Jiang, L. Yang, C. Li, C. Yan, P. S. Lee, and J. Ma, *Energy Environ. Sci.*, 4 (2011) 1813.
26. M. Huang, Y. Hou, Y. Li, D. Wang, and L. Zhang, *Des. Monomers Polym.*, 20 (2017) 505.
27. A. Singh, S. Suri, P. Kumar, B. Kaur, A.K. Thakur, V. Singh, *J. Alloys Comp.*, 764 (2018) 599.
28. P. Pascuta, L. Pop, S. Rada, B. Maria, C. Eugen, *J. Mater. Sci. Mater. Electron.*, 19 (2008) 424.
29. M. Jana, S. Saha, P. Khanra, P. Samanta, H. Koo, N. C. Murmu, and T. Kuila, *J. Mater. Chem. A*, 3 (2015) 7323.
30. J. J. Licari and D. W. Swanson, *Adhesives Technology for Electronic Applications* (2005) DOI: 10.1016/B978-081551513-5.50009-7.
31. A. A. Łatoszyńska, P. L. Taberna, P. Simon, W. Wieczorek, *Electrochim. Acta*, 242 (2017) 31.
32. M. Areir, Y. Xu, D. Harrison, J. Fyson and R. Zhang, *Mater. Manuf. Process.*, 33 (2018) 905.
33. H. Sun, X. Fu, S. Xie, Y. Jiang, and H. Peng, *Adv. Mater.*, 28 (2016) 2070.